Conical fluorescence emission from sodium vapor excited with tunable femtosecond light pulses

V. Vaičaitis and E. Gaižauskas
Laser Research Center, Vilnius University, Sauletekio 10, Vilnius LT-10223, Lithuania
(Received 4 July 2006; published 16 March 2007)

An experimental and theoretical investigation is made of the angular spectrum of a near-resonant femtosecond laser pulse propagating through sodium vapor. A directional fluorescence emission corresponding to single-photon sodium transition $3S \rightarrow 3P_{1/2,3/2}$ has been registered for the pump wavelength ranging from 540 to 605 nm. It is found that such emission can be detected under the conditions of single-photon (enhanced by two-photon) resonance of pump frequency with relevant atomic states. Theoretical treatment of the field-matter interaction by means of the nonperturbative (semiclassical) approach revealed conical components of the cylindrically symmetric beam spectrum originating both from the fluorescence induced by coherent atomic polarization and four-wave mixing.

DOI: 10.1103/PhysRevA.75.033808 PACS number(s): 42.65.Re, 42.50.Md, 42.62.Fi, 32.70.Jz

I. INTRODUCTION

The propagation of strong near-resonant light beams through an atomic vapor may induce so-called conical emission (CE). Usually redshifted in respect to the pump CE is observed for the frequency of laser beams close to but greater than that of the atomic resonance transition. Since the observation by Grischkowsky [1], this phenomenon has been studied widely both experimentally and theoretically (see, e.g., Refs. [2,3], and references therein). Nevertheless, there is still no generally accepted theory of this phenomenon regarding the causes and behavior of CE in atomic vapors. Most theories of CE are based on four-wave parametric amplification of redshifted Rabi sidebands generated in self-trapped filaments [4,5]. This approach proved to be quite successful for the case of continuous wave (cw) pumping when Valley *et al.* [6] described conical emission as an interplay between four-wave mixing and the effects of diffractive spreading during propagation. Nevertheless, even though in most cases the cone angle of CE calculated according to the models mentioned above is in agreement with the experimental data, there were reports [7,8] indicating the absence of the fourth blueshifted wave, associated with four-wave mixing (FWM). In addition, some experiments with pulsed lasers yielded other controversial results, such as the CE induced by a red-detuned pump beam, that are not consistent with FWM [9,10].

Therefore several alternative models have been proposed. The most relevant processes that have been invoked are stimulated Raman scattering [11], self-phase modulation [12], temporal pulse reshaping of Rabi sidebands [13,14], cooperative fluorescence [15,16], superfluorescence [17], and Cherenkov emission [18,19]. However, none of these models have been widely accepted. This fact supports the idea that the process of formation and propagation of CE is a complicated one and cannot be explained straightforwardly. Therefore most of the latest models include several different effects as well as the competition between these processes [6,16,20]. Nevertheless, under certain experimental conditions one or two processes could be clearly distinguished from the others. For example, the excitation of nonlinear media by ultrashort light pulses could reduce or even exclude thermal effects, while the pump frequency tuning allows one to modify the efficiency of resonant interactions. Nevertheless, so far in most of the experiments CE has been observed from nanosecond pulses and cw beams. However, there were a few reports of CE from ultrashort laser pulses [3,21,22], including the recent paper by Aumiler *et al.* [22] where the authors clearly demonstrated CE as being a result of self-phase modulation of femtosecond laser pulses in cesium dimers. Since their experimental conditions significantly differed from those of the previous experiments (high density of dimers, comparably low power density and high repetition rate of laser pulses), it further confirms the assumption that under the particular experimental conditions one or the other effect responsible for the generation of conical emission might dominate.

It is the purpose of this work to demonstrate both experimentally and by numerical calculations that, among the processes capable of producing CE, the fluorescence from a coherently excited two-level quantum system also should be considered. Specifically, we analyzed the spectral and spatial properties of sodium emission induced by femtosecond light pulses of different wavelengths. We have found that the experimentally observed conical part of radiation emitted near the single-photon sodium resonance transition $3P \rightarrow 3S$ can be attributed to fluorescence emission from resonantly and coherently excited polarization of sodium atoms. These findings were further confirmed by numerical analysis of the Bloch equation in two-level approximation. The study is motivated by the remarkable contradictions in treatment of conical radiation emitted from the resonantly excited atoms.

II. EXPERIMENT

For the excitation of sodium the optical parametric generator (OPG) pumped with the femtosecond Ti:Sapphire laser (Spitfire, Spectra Physics, Ltd) beam (wavelength about 800 nm, pulse duration about 120 fs, repetition rate 1 kHz, single pulse energy 2.3 mJ) has been used. The OPG produced visible output with the single pulse energy of about 0.05 mJ and spectral width varying between 140 and 300 cm^{-1}. The beam diameter was about 4 mm and since as a rule during the experiments for sodium excitation we did

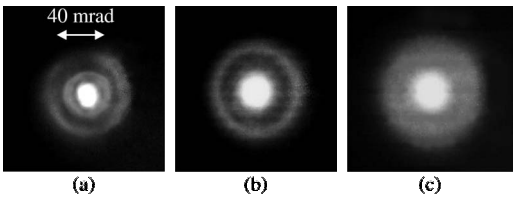

FIG. 1. Typical experimentally registered angular distributions of the emission generated in sodium vapor cell for the pump wavelength of (a) 567.5, (b) 581.5, and (c) 585.5 nm. Sodium density was 6×10^{15} cm^{-3}.

not use any collimating optics, the typical values of the power density of the pump beam in the sodium cell were evaluated as 0.5–4 GW/cm^2. At such high pump intensities, especially in the near resonance case of excitation, the efficient multiphoton ionization (MPI) of the media takes place. Thus, Lucatorto and McIlrath [23,24] have shown that irradiation of a dense column of Na vapor with a submicrosecond dye laser tuned to a D line can cause complete ionization of the vapor. However, the process of MPI of gases by femtosecond laser pulses is quite complicated and differs from that induced by longer pulses [25–28]. Thus, Jones [28] has shown that the probability of MPI of sodium atoms excited with femtosecond light pulses is quite low as long as the pump power density does not exceed tens of GW/cm^2. Also, the straightforward estimation of sodium ionization degree from the excited $3P$ level for the typical value of two-photon photoionization cross section of 10^{-48} cm^4 s [29] gives similar results even assuming the full saturation of the sodium $3P$ level. Nevertheless, though for the excitation of sodium vapor the comparably low power density beam has been used, we believe that during our experiments the degree of sodium ionization varied significantly and in some cases could reach up to a few tens of percent.

The sodium cell was made from stainless steel with two room temperature windows. The center of the pipe could be heated to temperatures up to 550 °C. A further increase of the temperature led to the increased sodium dimer absorption and broadened atomic resonance lines [30]. The length of the heated section of the cell was 15 cm and its temperature was monitored with thermocouples. Pressure of the Ar buffer gas was about 10 Torr at room temperature of the heated section. Since the lowest-energy single-photon transitions from the ground state of argon lie in the vacuum UV, we have assumed that its presence should not influence significantly the effects observed in a visible spectral region.

The radiation emerging from the sodium cell was imaged either on a screen or sent to the input of the spectrometer (Ocean Optics, Inc). The patterns emerging on the screen were registered with the help of a charge-coupled device (CCD) camera. A set of optical filters was used to prevent overexposure of the camera as well as to select desirable wavelength of the registered signal. The typical patterns of experimentally registered radiation emitted from sodium vapor are presented in Fig. 1. In general the transmitted light is seen to consist of a bright central spot surrounded by a diffuse ring (corresponding to the pump beam and CE, respectively). Conical fluorescence emission had a large angular

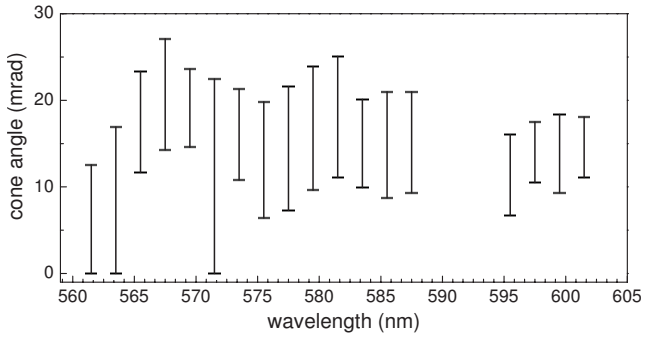

FIG. 2. Dependence of CE cone half-angle on the pump wavelength at sodium density of about 2×10^{15} cm^{-3}. The vertical bars (to be distinguished from the error bars) represent the experimentally measured minimum and maximum angle values.

spread $\Delta\theta/\theta$ ranging from 0.4 to 1. For the blue-detuned pump, however, the additional narrower cone of broadband light could be seen [Fig. 1(a)]. The spectral and angular properties of this radiation were clearly distinct from that of fluorescence emission [31]. The source of such broadband CE was identified as FWM enhanced by the ac-Stark effect and will be reported elsewhere.

The directional fluorescence emission in the visible spectral region has been observed for sodium densities ranging from 5×10^{13} to 2×10^{16} cm^{-3} and for the pump red or blue detuned from the atomic resonance $3S\rightarrow3P$. The tuning range to the blue (high-frequency) side was significantly wider than that to the red (low-frequency) side and has been estimated to be 1500 and 400 cm^{-1}, respectively. This corresponds to an overall tuning range between 540 and 605 nm. Therefore the pump beam could be tuned through the two-photon sodium resonances $3S\rightarrow4D$, $3S\rightarrow5S$, and $3S\rightarrow6S$. In addition, the pump beam frequency always remained near the single-photon sodium resonance $3S\rightarrow3P$. Outside that pump wavelength range no directional fluorescence emission has been detected. We also could not see any backward emission in the visible spectral region for the pump tuning range mentioned above. Though conical fluorescence emission has been detected in the whole pump tuning range, CE was more pronounced for the pump tuned near two-photon resonance with relevant sodium states. The color of emitted light was always yellow with a wavelength close to that of the sodium resonance doublet.

The angular structure of the fluorescence emission was strongly dependent on the pump wavelength and on the density of sodium vapor. While the average cone angle increased with increasing sodium vapor density, it remained almost constant over the whole pump tuning range. However, the angular spread $\Delta\theta/\theta$ of the cone was strongly dependent on the pump wavelength (Figs. 1 and 2). Likewise, the average cone angle was found to be independent of input beam intensity, whereas its angular spread increased with the pump power. Note that when the pump was in resonance with sodium transition $3S\rightarrow3P$ at about 589 nm, the angular structure of the conical emission could not be registered, due to the high divergence of the transmitted pump beam and the proximity of its wavelength to that of the fluorescence light.

The typical spectra of the fluorescence emission are presented in Figs. 3 and 4. In general the spectral structure of

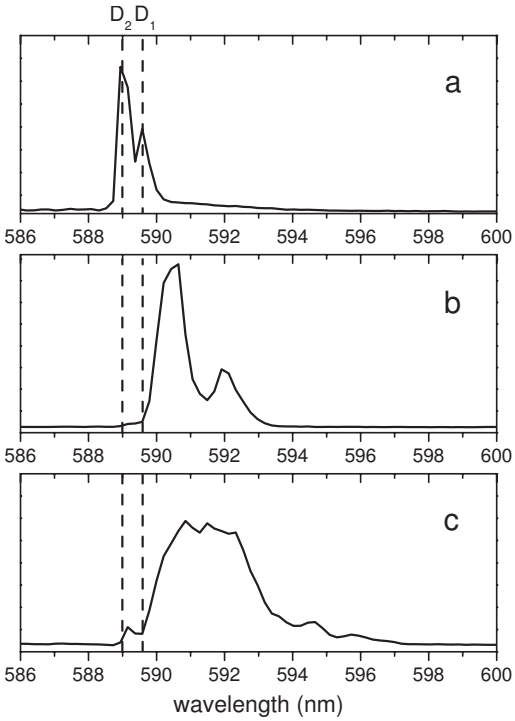

FIG. 3. CE spectra at pump wavelength of 571 nm and sodium density of (a) 5×10^{14}, (b) 7×10^{15}, and (c) 10^{16} cm^{-3}. The two vertical dashed lines correspond to wavelengths of the sodium resonance doublet.

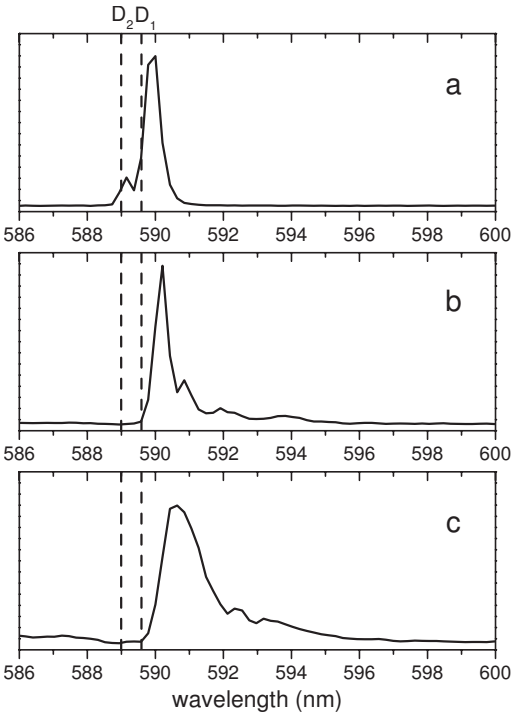

FIG. 4. CE spectra at pump wavelengths of (a) 551, (b) 576, and (c) 585 nm. The sodium vapor density was 10^{16} cm^{-3}.

generated emission remained constant over the entire range of pump frequencies and consisted of two peaks with different intensities. In most cases the separation of these two components did not vary with pump detuning and was similar to that of the sodium resonance doublet within the accuracy of the experiment. In addition, at low sodium densities and large pump detunings from the resonance the wavelengths of these two peaks corresponded to the sodium resonance doublet $3P_{1/2,3/2}\rightarrow 3S$ [Fig. 3(a)]. However, at high sodium densities these peaks merged together into a single one [Fig. 3(c)]. Note that at high sodium vapor densities the D lines of sodium overlap each other in a similar way. These findings further support the idea that the origin of observed conical emission is closely related with the resonance fluorescence.

We have also found that the spectral width of the emission increases with sodium density, but is almost independent of the pump wavelength. However, at high sodium densities the spectrum of CE broadened and shifted slightly to the red [Fig. 4(c)] when the pump detuning from sodium resonance $3S\rightarrow 3P$ was decreased.

Therefore in general at high sodium densities the cone peak wavelength lies on the red side of sodium resonance transition $3S\rightarrow 3P_{1/2}$ (wavelength about 590 nm) and shifts further to longer wavelengths as the density of sodium increases. Typically, the peak of the CE spectrum was detuned from resonance by 2.5–10 cm^{-1} for the density of sodium vapor of 2×10^{15} cm^{-3}.

We have also noticed the increase of the spectral width of CE when the pump beam was focused into the center of the sodium cell. The typical spectra of this emission obtained using the focused and unfocused pump beams are presented in Fig. 5. It is clearly seen that the spectral width of CE increases with the pump intensity. Note that this effect was more pronounced at higher sodium densities.

III. MODEL AND CALCULATION PROCEDURE

Despite extensive research in the area of the interaction of coherent optical pulses with a collection of two-level atoms, only a few theoretical studies have investigated the changes in the spectrum of a femtosecond pulse as it propagates through a resonant atomic medium. Recently the spectral behavior of a broadband coherent pulse was analyzed in the plane-wave limit, demonstrating spectral signatures of the ac-Stark shifts in thin samples [32]. Here we analyze the changes in the angular spectra (i.e., spectral changes versus

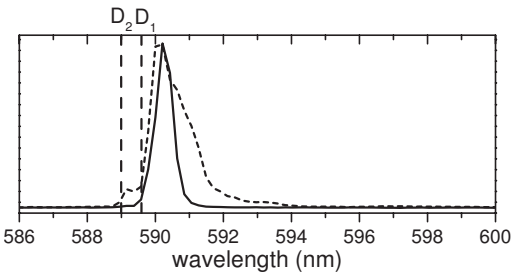

FIG. 5. CE spectra at pump wavelength of 566 nm and sodium vapor density of 7×10^{15} cm^{-3}. The intensity of the input laser beam was estimated to be about 4 and 40 GW/cm^2 (solid and dashed curves, respectively).

transversal wave number $k_\perp$ in the beam) of the femtosecond wave packet. The motivation for the numerical investigation of the problem is (1) no one of the limiting cases (in which the analytical expression for induced polarization can be obtained) can be attributed to our purpose and (2) the principal point for the proper treatment of the angular spectra is to account for the field-affected spectral distribution of the excitations in an ensemble of quantum systems (dressed-atom spectra).

Consider a localized two-level quantum system, characterized by resonance transition frequencey ω_{21} and subjected to the femtosecond laser (pump) pulse. In contrast to plane-wave analysis provided in [32], we model the linearly polarized beam with cylindrical symmetry around the propagation axis z by the envelope $\mathcal{E}$ of the electric field $\mathbf{E}$, written as $\mathbf{E}=\mathrm{Re}[\mathcal{E}\exp(ikz-i\omega_L t)]$, where $k=\omega_L/c$ and ω_L are the wave number and frequency of the carrier wave. In our model we analyze the spectral properties of the emitted radiation.

The scalar envelope $\mathcal{E}(r,t,z)$ evolves along the propagation axis z according to the three-dimensional wave equation governing propagation of the pulse in a medium with an atomic density N:

$$\frac{\partial \mathcal{E}}{\partial z} - i\frac{1}{2k}\nabla_\perp^2 + \frac{1}{c}\frac{\partial E}{\partial t} = \frac{4\pi\omega N\mu}{\hbar c}Q, \tag{1}$$

where $Q(r,t,z)$ denotes slowly varying amplitude of the high-frequency polarization induced in the quantum ensemble of the atoms. After introducing the Rabi frequency for the pulse envelope $\Lambda(r,z,t)=2\mu\mathcal{E}/\hbar$, the Bloch equation for the complex polarization Q and population difference w in the two-level system reads

$$\frac{\partial Q}{\partial t} = -\left(\frac{1}{T_2} - i\Delta_L\right)Q + \frac{i}{2}\Lambda_L w, \tag{2}$$

$$\frac{\partial w}{\partial t} = -i(\Lambda_L Q^* - \Lambda_L^* Q) - \frac{1+w}{T_1}, \tag{3}$$

where $\Delta_L=\omega_L-\omega_{21}$ and T_1, T_2 stand for the population and polarization relaxation, respectively. The field frequencies are considered as being near to the resonance of the optical transition of the system. Actually, resonance condition means that $\Delta_L \ll \omega_{21}, \omega_L$. Thus, we have used the rotating frame approximation and excluded the dominant time dependence $\sim\exp -i\omega_L t$ in Eqs. (2) and (3). It should be noted that this type of the light-matter interaction strongly depends on the relations between frequency offset Δ_L from the resonance, the linewidth of quantum system $1/T_2$, and the pump pulse bandwidth, which is the inverse of pulse duration. Fulfilling condition $1/t_p \geqslant \Delta_L \approx 1/T_2$ can be defined as the case of coherent resonance, whereas the opposite $(1/t_p \approx \Delta_L \ll 1/T_2)$ is characteristic for (resonant but) incoherent interaction. In the intermediate case, when $\Delta_L \gg 1/t_p$ and $1/t_p \leqslant 1/T_2$, adiabatic following of the polarization is characteristic for the system, though long lasting coherences (decaying with time constant T_2) still remain after the pump is switched off. Numerical analysis of Eqs. (1)–(3) is required in order to cover all cases described above.

Equations (1)–(3) account for the variety of effects: diffraction in the transverse plane, group velocity dispersion, and self-action due to the nonlinear polarization induced in the two-level quantum system. Nevertheless, for the pump beam waist $w_0=1$ mm and the length of the interaction $L=5$ cm used in our numerics, the spatial structure of the emitted (conical) radiation results mainly from the effects, emerging due to the finite memory of induced nonlinear polarization.

To split the problem into propagative and nonlinear parts we have used a generalized split-step procedure and solved the appropriate equations inside each step separately. A finite difference method for Eq. (1) was used to propagate wave packets along the z coordinate. After that to Eqs. (2) and (3) we applied the Runge-Kutta method of the fourth order to simulate the changes in time of the material variables. The time step was taken small enough to treat the change in the femtosecond time scale both for material variables Q, w and field E. In addition, the overall integration time interval was much longer than the system phase memory relaxation time (taken as 5 ps) to ensure that the coherent emission from excited polarization in the quantum system was accounted for.

In order to compare the results of numerical calculations with the experimental measurements (when on-axis radiation was filtered out), we have made the following approximation. Assuming that the intensity changes of the spatial spectra of investigated radiation are small, we propagated the probe wave packet through the sample by means of Eq. (1), whereas for the calculation of changes of material variables according to Eqs. (1)–(3) both wave packets (pump and probe) were used.

The input field at the entrance of the nonlinear medium was modeled by Gaussians [full width at half maximum (FWHM) duration $\tau_{FWHM} \equiv t_p\sqrt{2\log_e(2)}$]:

$$\mathcal{E}(r,t,0) = \mathcal{E}_{L,P}\exp\left(-\frac{r^2}{w_0^2} - \frac{t^2}{t_p^2}\right), \tag{4}$$

with the ratio $\mathcal{E}_\mathcal{P}/\mathcal{E}_\mathcal{L}=0.001$ of the probe and pump amplitudes.

IV. RESULTS OF NUMERICAL MODELING

The (2+1)-dimensional approach of the light-matter interaction described above allowed us to investigate the angular structure of generated emission along with its spectral properties. The changes of the angular spectra were obtained by Fourier-Hankel transform of the generated radiation $\mathcal{E}_\mathcal{P}(r,t,z)$ and depicted in $k_\perp-\lambda$ space.

It is instructive to start the analysis of femtosecond pulses propagating in the two-level quantum system by demonstrating its peculiarities on the pump wavelength. Therefore in Figs. 6 and 7 we plotted the angular spectra of generated radiation for the pump parameters $t_p=130$ fs, $\theta_L=5\pi$, and wavelengths of 575, 585, and 605 nm. The field amplitude was propagated for the distance L equal to 5 cm by taking absorption coefficient $\alpha=8\pi\mu^2\omega_{21}NT_2/\hbar c=130\ \mathrm{cm}^{-1}$. In order to match the parameters of our model with that of physi-

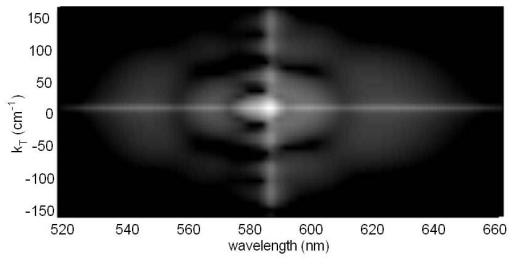

FIG. 6. Angular (calculated in $k_\perp - \lambda$ space) spectra of the generated radiation in 5 cm long sample of the media of two-level quantum systems having resonance at 589 nm. The wavelength of pump pulse $\lambda_L = 585$ nm. Other parameters: $\Lambda_0 = 5\pi$, $T_2 = 2$ ps, $T_1 = 1$ ns, $\alpha = 130$ cm^{-1}.

cal media used in the experiment (near-resonant excitation of sodium transition $3S \rightarrow 3P$), the value of $\lambda_{21} = 589$ nm was chosen as the resonance wavelength of the quantum system.

The distinct cones of the radiation at the resonant wavelength (589 nm) can be seen in all cases depicted in Figs. 6 and 7. Note that when the wavelength of the pump is tuned in close vicinity to the resonance ($\lambda_L = 585$ nm), the patterns of angular spectra (shown in Fig. 6) exhibit significant broadening both in space and wavelength. This is in accordance with the experimental observations [shown in Fig. 1(c)], where the blurred cones were observed for the case of near-resonant sodium excitation. Conversely, when the pump wavelengths have been detuned from the resonance [567 and 581 nm in Figs. 1(a) and 1(b)] the sharp rings were clearly visible. These sharp rings are also characteristic for the numerically obtained angular spectra shown in Fig. 7 (top) and obtained for the pump wavelength $\lambda_L = 575$ nm. The clear angular gap in this spectrum is easily seen despite the broadband on-axis radiation centered at the wavelength of the pump pulse and the one related with the broadband four-

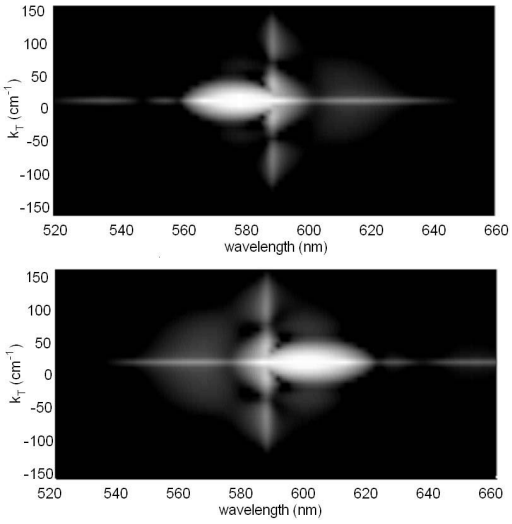

FIG. 7. Angular (calculated in $k_\perp - \lambda$ space) spectra of generated radiation, when the laser pulse of 200 fs duration was propagated at 5 cm distance in media of two-level quantum systems resonant at 589 nm. Pump pulse wavelength was 575 (top) and 605 nm (bottom). $\Lambda_0 = 5\pi$, $T_2 = 2$ ps, $T_1 = 1$ ns, $\alpha = 130$ cm^{-1}.

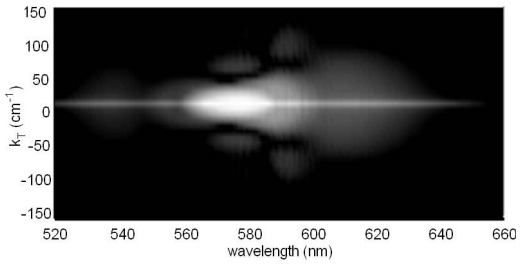

FIG. 8. Angular (calculated in $k_\perp - \lambda$ space) spectra of generated radiation in media of two-level quantum systems having the coherence relaxation time comparable to the pulse duration. Other parameters are the same as in Fig. 7 (top).

wave mixing. It should be noted that the case of pump wavelength $\lambda_L = 575$ nm corresponds to the "intermediate" excitation condition, as described above, when $\Delta_L \gg 1/t_p$ and $1/t_p \leqslant 1/T_2$. Indeed, in this case the offset from the resonance exceeds 400 cm^{-1} and becomes twice as large as the pump bandwidth. When the pump wavelength was tuned to the red side from the resonance ($\lambda_L = 605$ nm), the main features of the numerically obtained angular spectrum, depicted in Fig. 7 (bottom), remained practically the same as in the case discussed above ($\lambda_L = 575$ nm).

In order to clear out the role of coherence in light-matter interaction, in Fig. 8 we show numerically obtained angular spectra produced with phase relaxation time $T_2 = 0.2$ ps, i.e., ten times shorter compared to that used in Fig. 7. Note, nevertheless, that even in this case a small amount of coherent polarization should be present, as far as its relaxation time is comparable to the pump pulse duration. As it was expected, the short coherence relaxation time strongly affected conical radiation at the resonance frequency: it was spectrally broadened and suppressed considerably. We note here (in Fig. 8) the appearance of conical radiation at the pump wavelength which was not seen in the case of longer coherence constants.

V. DISCUSSION

As it was mentioned above, some properties of the investigated emission (two peaks with the separation identical to the one between sodium D_1 and D_2 lines, spectral width broadening with sodium density, insensitivity of the spectral features on pump wavelength, etc.) led us to the conclusion that the origin of CE is the resonance fluorescence from excited sodium atoms. However, in most cases the peak wavelengths of the experimentally registered emission were shifted to the red for a few cm^{-1} from the corresponding central wavelengths of sodium resonance lines D_1 and D_2 (589.59 and 588.99 nm, respectively). In addition, the clearly seen conical distribution of generated radiation suggests that there are involved some additional processes responsible for phase matching, since the fluorescence signal usually is emitted uniformly in every direction. However, it has been shown in [15] that the cooperative fluorescence radiation from collections of spatially distributed atoms could produce a cone-shaped emission. Note that in a field of strong pump pulse

the ac-Stark effect broadens atomic energy levels. Therefore if the nonlinear interaction takes place during the pump pulse propagation in media, the frequency of generated radiation should be shifted from the resonance by the amount of generalized Rabi frequency $\tilde{\Lambda}=\sqrt{\Omega^2+\Delta_L^2}$. Since in the media pump pulse intensity varies from zero to its maximal value, the resulting frequency shift should be time dependent and as a consequence a broadband radiation should be generated. For our experimental conditions and assuming no self-focusing of the pump beam the generalized Rabi frequency is much more ($300-1300\ \mathrm{cm}^{-1}$) than the shift in the wavelength of the fluorescence light ($5-10\ \mathrm{cm}^{-1}$). This result indicates that the ac-Stark shifts during pump propagation could not be responsible for the shift of CE wavelength. To overcome this contradiction, Shevy and Rosenbluh [33] suggested that the CE could be generated from the regions where the pump intensity is lower and the Rabi shifts are smaller, resulting in an emission close to the unperturbed atomic resonance frequency. This also seems unlikely as for the case of the unfocused pump beam the volume from which conical emission could be emitted would be significantly reduced, thereby reducing the efficiency of generation. On the other hand, since the Stark effect is a very fast phenomenon, due to the fact that for the case of ultrashort laser pulses the characteristic sodium fluorescence decay time is much longer than the pump pulse duration, only a small fraction of the fluorescence photons can be emitted from the perturbed atoms. Therefore, even if the fluorescence was emitted from the zone of perturbed sodium atoms, the contribution of the Stark effect to the spectrum of CE would be negligible.

The small shifts of sodium energy levels, however, also can be induced by resonantly created plasma due to the quadratic Stark effect in a microfield of ionized atoms and electrons [34–36]. The atomic line shifts induced in this way could be of the order of a few cm^{-1} [36], which well correspond to our experimental findings. This effect could also explain the experimentally observed broadening and shifting to the red of the cone spectrum when the pump intensity and sodium density increases or the pump wavelength is tuned to the single-photon sodium resonance $3S\rightarrow 3P$ (see Figs. 3 and 4): in all cases the number of ionized particles as well as the electric field strength created by them increases, thus increasing the quadratic Stark effect.

Though the spontaneous fluorescence is an incoherent phenomenon and is emitted randomly over 4π steradians, it has been shown [37] that when a quasiresonant light pulse with a duration of comparable with or shorter than the relaxation time of the atomic polarization is incident in the vapor, the atoms are emitting coherently like a phased-array radar. As a result, directional fluorescence emission could be generated. When the pump pulse velocity v_p and thus the velocity of the source of polarization is larger than that of the emitted fluorescence light v_f, due to the Cherenkov-type phase-matching process, the coherent superposition of all light fields will result in an emission of CE with a characteristic cone angle α given by $\cos\alpha=v_f/v_p$. Note that the Cherenkov-type phase matching is quite a common phenomenon and occurs during most of the nonlinear optical processes [38,39], whenever the velocity of the light source exceeds that of the emitted radiation.

The large angular width of generated CE could be explained by the proximity of the cone spectrum to the resonance frequency of unperturbed sodium atoms. In this spectral region cone angle strongly depends on its wavelength because of the steep slope of the refractive index as a function of frequency. Therefore the spread of the cone angle is large, in spite of the narrow frequency spectrum of CE. In addition, the spatial structure of the cooperative fluorescence radiation is very sensitive to the correlation length of coherently excited atoms: the shorter the correlation length, the more diffuse CE is generated. In the limit of infinitely short correlation lengths excited atoms decay independently of one another and emit randomly phased light which is scattered equally in all directions. [Figures 7 (top) and 8 illustrate this phenomenon: CE is clearly seen for the phase relaxation time T_2 taken as 2 ps, while it is almost unnoticeable when $T_2=0.2$ ps.]

The radiation emitted from sodium atoms slightly perturbed by plasma microfields is reabsorbed by other perturbed atoms along the pump beam path. Therefore the spatial components of conical emission propagating close to the pump direction are absorbed stronger than those directed off axis. On the other hand, the frequency components that are close to resonance and propagate at some angle to the direction of the pump can be absorbed by unperturbed atoms more than propagating along the saturated pump beam path. This effect can increase the cone angle and significantly modify the spatial and spectral structure of emitted radiation. It may also be significant in explaining the fact that in most cases the CE is well separated spatially from the laser beam.

In addition, the conical nature of the fluorescence emission appears also to be consistent with a refraction model in which radiation generated in nearly saturated regions of the atomic vapors refract out of these regions in the form of a cone [40]. This effect can also increase the angle of CE emitted from saturated regions of sodium vapor.

Under the conditions of single- and two-photon resonances, which was the case during our experiments, the efficient parametric four-wave mixing (PFWM) and other nonlinear optical processes take place. The radiation of resonantly enhanced PFWM has been observed near the frequency of sodium transition $3S\rightarrow 3P$, in a region where large refractive index dispersion is present and, thus, the phase matching conditions are satisfied [41]. The light generated through such a process usually has a conical form and the wavelength redshifted from sodium resonance transition $3S\rightarrow 3P$, therefore the PFWM should be always considered as the possible source of CE [4,5]. However, the fluorescence and PFWM emissions have different spatial and spectral properties, which allow the processes to be unambiguously distinguished. There is, however, the possibility that the weak fluorescence lines are amplified through the process of four-wave mixing. This effect could be important when the phase matching conditions are fully satisfied. Note that the idler wave generated during such an amplification process should also have the form of a cone. However, during our experiments we did not observe any conical emission at a frequency of the idler wave.

The main competing process capable of reducing the efficiency of the coherently excited fluorescence is the multiphoton ionization. During our experiments the wavelength of the pump has been tuned over a wide spectral range including single- and two-photon resonances of sodium. Assuming the complex dependence of MPI on the pump intensity and media properties, the quantitative evaluation of the number of ionized atoms is a complicated task. However, though in some cases this process is capable of ionizing up to 100% of atoms, in general it could influence the properties of CE only quantitatively. First, the MPI could decrease the number of excited neutral atoms and thus reduce the efficiency of the fluorescence. Second, the large amount of ionized particles could modify the refraction index of the media significantly, consequently influencing the phase matching conditions for the nonlinear optical processes involved into consideration. Therefore, we believe that during our experiments the MPI manifests itself mainly by modifying the angular structure of CE (see Figs. 1 and 2 showing the dependence of the cone angle and its half-width on the pump wavelength). Also, as we discussed above, the frequency shift and increase of the spectral width of registered conical fluorescence emission could be directly related with the ionization degree of sodium atoms.

In the present experiment the detuning from resonance and spectral width of CE, which was $5-10\ \mathrm{cm}^{-1}$, seems to be very close to the values obtained in most of the nanosecond experiments at similar sodium densities. Therefore we suppose that our experimental results further support the idea that the directional fluorescence emission from coherently excited atoms [15,37] can be considered as an origin of previously reported CE in at least some cases. However, in the present case the pump intensity was significantly higher, thus inducing the larger Stark shifts as well as the higher level of sodium ionization. In addition, during our experiments, due to its wide spectral width a significant fraction of the pump pulse was in resonance with the single- and two-photon transitions of sodium, thus additionally increasing the ionization level of the vapor.

VI. CONCLUSIONS

We have shown that conical fluorescence emission is efficiently generated in sodium vapor excited with tunable femtosecond light pulses. This visible emission corresponding to single-photon sodium transition $3S \rightarrow 3P_{1/2,3/2}$ has been registered experimentally for wide sodium density (from 5×10^{13} to $2\times10^{16}\ \mathrm{cm}^{-3}$) and pump wavelength (between 540 and 605 nm) range. The spectral and spatial properties as well as the behavior of this emission as a function of laser intensity and detuning from sodium resonance indicate that the cone is produced by a cooperative fluorescence from collections of atoms with shifted energy levels due to the quadratic Stark effect in a microfield of ionized atoms and electrons. The cone angle of this emission is determined by the Cherenkov phase-matching process which takes place in the case of coherent excitation of sodium atoms. However, several other effects can modify additionally the spatial and angular structure of emitted radiation, including the resonant absorption of conical signal and refraction of light from the saturated regions of sodium where CE is generated. In summary, the similarity of the features of conical emission obtained in the present and in most of the previous experiments with nanosecond laser pulses suggests that at least in some cases the registered CE could be caused by the cooperative fluorescence emission from coherently excited atoms. However, under the resonant conditions strong FWM, which has been registered experimentally and confirmed by numerical calculations, also takes place. Therefore the coherently excited fluorescence is one of the processes capable of producing CE and should be taken into account in the future investigations of this phenomenon.

ACKNOWLEDGMENTS

This work was supported by NATO Collaborative Linkage Grant No. PST.CLG 980299 and the Lithuanian State Science and Studies Foundation.

[1] D. Grischkowsky, Phys. Rev. Lett. **24**, 866 (1970).
[2] B. D. Paul, J. Cooper, A. Gallagher, and M. G. Raymer, Phys. Rev. A **66**, 063816 (2002).
[3] D. Sarkisyan, B. D. Paul, S. T. Cundiff, E. A. Gibson, and A. Gallagher, J. Opt. Soc. Am. B **18**, 218 (2001).
[4] D. J. Harter and R. W. Boyd, Opt. Lett. **7**, 491 (1982).
[5] D. J. Harter and R. W. Boyd, Phys. Rev. A **29**, 739 (1984).
[6] J. F. Valley, G. Khitrova, H. M. Gibbs, J. W. Grantham, and Xu Jiajin, Phys. Rev. Lett. **64**, 2362 (1990).
[7] C. H. Skinner and P. D. Kleiber, Phys. Rev. A **21**, 151 (1980).
[8] B. D. Paul, M. L. Dowell, A. Gallagher, and J. Cooper, Phys. Rev. A **59**, 4784 (1999).
[9] R. C. Hart, L. You, A. Gallagher, and J. Cooper, Opt. Commun. **111**, 331 (1994).
[10] J. Pender and L. Hesselink, J. Opt. Soc. Am. B **7**, 1361 (1990).
[11] A. C. Tam, Phys. Rev. A **19**, 1971 (1979).
[12] M. L. Ter-Mikaelian, G. A. Torossian, and G. G. Grigoryan, Opt. Commun. **119**, 56 (1995).
[13] M. E. Crenshaw and C. D. Cantrell, Opt. Lett. **13**, 386 (1988).
[14] M. E. Crenshaw and C. D. Cantrell, Phys. Rev. A **39**, 126 (1989).
[15] W. Chalupczak, W. Gawlik, and J. Zachorowski, Phys. Rev. A **49**, R2227 (1994).
[16] L. You, J. Mostowski, and J. Cooper, Phys. Rev. A **46**, 2903 (1992).
[17] Y. Ben-Aryeh, Phys. Rev. A **56**, 854 (1997).
[18] I. Golub, G. Erez, and R. Shuker, J. Phys. B **19**, L115 (1986).
[19] L. You, J. Mostowski, J. Cooper, and R. Shuker, Phys. Rev. A **44**, R6998 (1991).
[20] E. A. Chauchard and Y. H. Meyer, Opt. Commun. **52**, 141 (1984).
[21] V. Vaichaitis, M. Ignatavichyus, V. A. Kudryashov, Yu. N. Pi-

menov, and N. D. Ustinov, JETP Lett. **45**, 414 (1987).
[22] D. Aumiler, T. Ban, and G. Pichler, Phys. Rev. A **71**, 063803 (2005).
[23] T. B. Lucatorto and T. J. McIlrath, Phys. Rev. Lett. **37**, 428 (1976).
[24] T. J. McIlrath and T. B. Lucatorto, Phys. Rev. Lett. **38**, 1390 (1977).
[25] M. P. de Boer and H. G. Muller, Phys. Rev. Lett. **68**, 2747 (1992).
[26] G. N. Gibson, R. R. Freeman, and T. J. McIlrath, Phys. Rev. Lett. **69**, 1904 (1992).
[27] G. N. Gibson, R. R. Freeman, T. J. McIlrath, and H. G. Muller, Phys. Rev. A **49**, 3870 (1994).
[28] R. R. Jones, Phys. Rev. Lett. **74**, 1091 (1995).
[29] C. Laughlin, J. Phys. B **11**, 1399 (1978).
[30] H.-K. Chung, K. Kirby, and J. F. Babb, Phys. Rev. A **63**, 032516 (2001).
[31] V. Vaicaitis, in *CLEO/QELS, 2005* (Optical Society of America, Washington, DC, 2005), JWB83.
[32] J. K. Ranka, R. W. Schirmer, and A. L. Gaeta, Phys. Rev. A **57**, R36 (1998).
[33] Y. Shevy and M. Rosenbluh, J. Opt. Soc. Am. B **5**, 116 (1988).
[34] M. Kettlitz and P. Oltmanns, Phys. Rev. E **54**, 6741 (1996).
[35] V. Milosavljevic, S. Djenize, and M. S. Dimitrijevic, Phys. Rev. E **68**, 016402 (2003).
[36] O. L. Landen, R. J. Winfield, D. D. Burgess, J. D. Kilkenny, and R. W. Lee, Phys. Rev. A **32**, 2963 (1985).
[37] J. Guo, J. Cooper, and A. Gallagher, Phys. Rev. A **52**, R3440 (1995).
[38] D. H. Auston, K. P. Cheung, J. A. Valdmanis, and D. A. Kleinman, Phys. Rev. Lett. **53**, 1555 (1984).
[39] V. Vaicaitis, Opt. Commun. **209**, 485 (2002).
[40] D. J. Harter, P. Narum, M. G. Raymer, and R. W. Boyd, Phys. Rev. Lett. **46**, 1192 (1981).
[41] R. K. Wunderlich, W. R. Garrett, R. C. Hart, M. A. Moore, and M. G. Payne, Phys. Rev. A **41**, 6345 (1990).